

# Aircraft Classification Method Based on EEMD and Multifractal Correlation

Junyong Hu<sup>1, 2</sup>, Qiusheng Li<sup>1, 2, \*</sup>, Qianli Zhang<sup>1, 2</sup>, and Jingran Su<sup>1, 2</sup>

**Abstract**—The research goal of low-resolution radar aircraft target classification is to analyze the category of the given low-resolution radar aircraft target echo. In existing solutions, the feature extraction methods based on rotating modulation spectrum have good performance, such as the complex cepstrum method, autocorrelation method, cycle diagram method, autoregressive model power spectrum method, and singular value decomposition method. Most of these methods are more complicated in calculations, and practical applications often require higher pulse frequencies and longer observation times, which are greatly restricted. In this paper, a classification method based on ensemble empirical mode decomposition and multifractal correlation (CMEEMDMFC) is proposed. The basic design idea is to obtain the intrinsic mode functions (IMFs) by using the signal decomposition ability of ensemble empirical mode decomposition (EEMD) and select some components which are beneficial for improving the signal-to-noise ratio (SNR) for recombination. Then extract the corresponding multifractal correlation (MFC) features from the new signals for recognition. For verifying the validity of the model, a comparison model was selected to test on the same data set. Experimental results show that the proposed model performs well in classification accuracy.

## 1. INTRODUCTION

Automatic radar target recognition has always been a hot topic in the related research field. At present, scholars have done much research on target recognition of high-resolution radar and achieved many results [1, 2]. However, these results do not apply to low-resolution radars [3]. Therefore, the research of low-resolution radar target recognition has practical significance and application value. Active airborne early warning radars are mostly traditional low-resolution systems. Due to system characteristics such as low repetition frequency, narrow system frequency band, and short target irradiation time, it has always been difficult to classify and identify targets on them. Aircraft has always been one of the crucial targets of low-resolution radar. The classification and recognition technologies of low-resolution radar targets are mainly embodied in the following two aspects: the target recognition technology based on the characteristics of the rotating modulation spectrum and the target recognition technology based on the doppler spectrum, among which the rotating modulation spectrum features are the most common [4, 5]. Most of the existing solutions require higher pulse repetition frequency and longer observation time, which are greatly limited in practical application [6].

In recent years, fractal has been widely used in recognition fields, such as iris recognition [7] and texture recognition [8]. The application of fractal to aircraft target recognition is also one of the research directions. According to [9] conventional low-resolution radar's classification and recognition effect can be achieved through fractals under specific experimental conditions. However, under the background of solid clutter, the function of the fractal is greatly affected. In [10, 11], the application of

---

*Received 12 July 2021, Accepted 1 September 2021, Scheduled 7 September 2021*

\* Corresponding author: Qiusheng Li (bjliqiusheng@163.com).

<sup>1</sup> Research Center of Intelligent Control Engineering Technology, Gannan Normal University, Ganzhou 341000, Jiangxi, China.

<sup>2</sup> School of Physics and Electronic Information, Gannan Normal University, Ganzhou 341000, Jiangxi, China.

multifractal (MF) and multifractal correlation (MFC) in aircraft target classification and recognition of low-resolution radar under a specific simulation environment is described. Zhang et al. [12] combined MF with the fractional Fourier transform and used fractional Fourier transform to adjust the signal to the domain with the largest SNR for analysis, thus obtaining a better classification and recognition effect. In [13], the fractal dimension of the signal extracted from the frequency domain is taken as the identification feature of the modulation of radar signal pulses. The recognition effect is good when the SNR is high, and the recognition effect is not good when the SNR is low. Chen et al. [14] extracted the fractal dimension of the signal from the bispectral transform domain of the signal as the classification and recognition feature. Then the classifier is used to realize the classification and recognition of the radar signal. However under the condition of a low SNR, the recognition effect is still not good. It can be seen that to better play the role of fractal theory, we must first improve the SNR. In this paper, we use the signal decomposition ability of ensemble empirical mode decomposition (EEMD) to get the IMFs and screen out the components conducive to utilizing the SNR for recombination. The second step is feature extraction, which extracts the corresponding MFC features from the new signal for recognition. Compared with the existing fractal algorithm, the performance of the algorithm is analyzed.

## 2. THEORETICAL BASIS

### 2.1. Ensemble Empirical Mode Decomposition

Empirical mode decomposition (EMD) decomposes the fluctuations and trends of different scales in the signal step by step to form a series of data sequences with different characteristic scales [15], namely the intrinsic mode function (IMF) EEMD is obtained by improving the EMD method [16], which solves the defect of EMD mode aliasing by adding evenly distributed white noise several times. The algorithm steps are as follows [17]:

(1) Let the original signal be  $f(t)$ , and set the amplitude of the added white noise as  $a$  and the overall average number of times as  $m$ .

(2) Add a white noise sequence with an amplitude coefficient of  $a$ :

$$f_m(t) = f(t) + a \cdot n_m(t) \quad (1)$$

where  $x_m(t)$  is the new signal obtained after adding the  $m$ 'th white noise to the original signal data, and  $n_m(t)$  is the white noise.

(3) The signal with white noise was decomposed into a series of IMFs by the EMD method. The component of the  $i$ 'th component response and the residual component is obtained.

(4) The series of IMFs obtained this time were calculated on average to get the final IMF. The calculation formula is as follows:

$$\overline{IMF}_i = \sum_{m=1}^N \frac{IMF_{i,m}}{N} \quad (2)$$

wherein  $\overline{IMF}_i$  is the  $i$ 'th component finally obtained,  $N$  the number of white noise sequences, and  $IMF_{i,m}$  the  $i$ 'th component after adding the  $m$ 'th white noise processing.

### 2.2. Multifractal Correlation

The MF spectrum which is used to reflect the macroscopic properties of the object is obtained by statistical analysis of the singularity intensity observed at any point on the branch set [18]. The MFC spectrum is obtained by statistical analysis of the probability of two given singularity intensities observed at two different  $D$  apart to reflect more information of the object [19]. MFC theory is based on MF theory, so its theoretical reasoning is closely related.

When calculating the MF spectrum, we first define the probability distribution of measure  $\mu$  in a certain region as  $P_i(\varepsilon)$ :

$$P_1(\varepsilon) \propto \varepsilon^\alpha \quad (3)$$

Besides, the fractal dimension of the graph defined from the measuring point of view is  $D_0$ :

$$D_0 = -\frac{\ln N_\varepsilon}{\ln \varepsilon} (\varepsilon \rightarrow 0) \quad (4)$$

Then

$$N_\varepsilon \propto \varepsilon^{-f(\alpha)} \tag{5}$$

Combined with formula (3) and formula (4), the following formula is obtained:

$$P_\varepsilon(\alpha) = \frac{N_\varepsilon(\alpha)}{N_\varepsilon} \propto \varepsilon^{D_0-f(\alpha)} \tag{6}$$

wherein  $f(\alpha)$  is an MF singular spectrum.

Similarly, the MFC spectrum  $\tilde{f}$  meets the following formula:

$$P_\varepsilon(\alpha_1, \alpha_2, d) \propto \varepsilon^{D_0-\tilde{f}(\alpha_1, \alpha_2, w)} \tag{7}$$

Herein,  $\alpha_1$  and  $\alpha_2$  are two given singularity intensities, and  $P_\varepsilon$  is the probability of two given singularity intensities observed at different positions of  $d$  apart. The formula of  $w$  is as follows:

$$w = \ln d / \ln \varepsilon \tag{8}$$

Based on the discontinuous measure generated by the random multiplication process, and according to the inference about MFC spectrum in literature it can be obtained as follows:

$$\tilde{f}(\alpha_1, \alpha_2, w) = \begin{cases} wf[\alpha(Q_1 + Q_2)] + (1 - w)\{f[\alpha(Q_1)] + f[\alpha(Q_2)] - D_0\}, & \phi(q_1, q_2) < 1 \\ f[\alpha(Q_1)] + f[\alpha(Q_2)] - D_0 - w, & \phi(q_1, q_2) > 1 \end{cases} \tag{9}$$

Among them, the intermediate function:

$$\phi(q_1, q_2) = \min\{\phi(q_1, q_2), 1\} = \min\{\tau(q_1, q_2) - \tau(q_1) - \tau(q_2) - D_0, 1\} \tag{10}$$

### 3. MULTIFRACTAL CORRELATION FEATURES

#### 3.1. System Structure

The structural diagram of the aircraft classification system in this experiment is shown in Fig. 1.

The specific process is as follows:

- (1) Conduct EEMD analysis on aircraft radar echo signals to obtain multiple IMFs.
- (2) Select appropriate IMFs for reconstruction to get new signals.
- (3) MFC analysis was carried out on the new signals, and appropriate features were selected.
- (4) The feature data set is divided into the training set and test set in a ratio of 1 : 4.
- (5) Do some statistical analysis of data.

#### 3.2. Selection of IMFs

Based on the empirical values of EEMD, set the two parameters ( $a$  and  $m$ ) mentioned in Section 2.1 as 0.2 and 100, respectively [20]. In this paper, radar echo data can be decomposed into ten components. In the process of component screening, the concept of waveform entropy [21] is introduced in this paper. For signal  $s$ , the waveform entropy is defined as:

$$Entropy(s) = - \sum_{i=1}^N p_i \log_2 p_i \tag{11}$$

Therein,

$$P_i = |s_i| / \sum_{i=1}^N |s_i| \tag{12}$$

$s$  is the signal with  $N$  values, and  $s_i$  is the  $i$ th value of the signal.

The waveform entropy can be used to evaluate the intensity of the waveform, and the waveform entropy can better distinguish the IMFs decomposed by EEMD [22]. Taking certain data as an example, the waveform entropy of each IMF obtained by EEMD decomposition is calculated, and the normalized

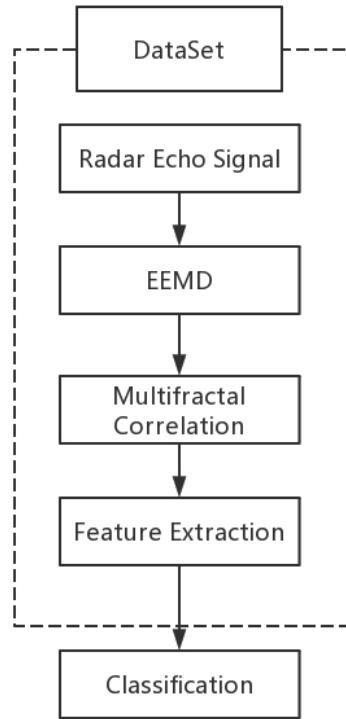


**Figure 1.** Schematic diagram of the aircraft classification system structure.

waveform entropy is 0.26, 1, 0.83, 0.53, 0.53, 0.44, 0.23, 0.35, 0.08, 0.16, respectively. In [23], the authors select the appropriate threshold value for selecting IMFs and get a good result. The method chosen in this paper is the same as described above, and the appropriate threshold value is selected for reconstruction. In the simulation experiment, the threshold values in different ranges were repeatedly set for solving. We observed that classification recognition effect was the best when the threshold value was in the interval  $[0.22, 0.85]$ . The signal was reconstructed according to the following IMFs (IMF<sub>3</sub>, IMF<sub>5</sub>, IMF<sub>4</sub>, IMF<sub>6</sub>, IMF<sub>8</sub>, IMF<sub>1</sub>, and IMF<sub>7</sub>).

### 3.3. Feature Selection

Feature selection has always been a difficulty in customizing features. In this paper, after combining with relevant literature, the following features are predetermined as classification features [24]:

- (1) Spectral barycenter

$$S_0 = \frac{\iint \sigma' |f(\sigma', \sigma'', w)|^2 d\sigma' d\sigma''}{\iint |f(\sigma', \sigma'', w)|^2 d\sigma' d\sigma''} \quad (13)$$

Since the MFC spectrum is symmetric concerning the plane  $\sigma' = \sigma''$ , the integral in the above expression can also be obtained to  $\sigma'$ , and the result is the same. The points  $(\sigma', \sigma'')$  describe the distributed barycenter of the MFC spectrum in the plane of  $\sigma' = \sigma''$ .

- (2) The maximum singularity index of the MFC spectrum

$$\sigma'_{\max} = \max(\sigma') \quad (14)$$

- (3) The minimum singularity index of the MFC spectrum

$$\sigma'_{\min} = \min(\sigma') \quad (15)$$

- (4) Spectral correlation width

$$\sigma'_{width} = \sigma'_{\max} - \sigma'_{\min} \quad (16)$$

(5) MFC spectrum distribution width ratio

$$R_f = \frac{\Delta\sigma_{LY}}{\Delta\sigma_{RY}} \tag{17}$$

In the formula,

$$\Delta\sigma_{LY} = f(\sigma_0, \sigma_0, w) - f(\sigma'_{\min}, \sigma'_{\min}, w) \tag{18}$$

$$\Delta\sigma_{RY} = f(\sigma_0, \sigma_0, w) - f(\sigma'_{\max}, \sigma'_{\max}, w) \tag{19}$$

(6) MFC spectral asymmetry index

$$R_\sigma = \frac{\Delta\sigma_L - \Delta\sigma_R}{\Delta\sigma_L + \Delta\sigma_R} \tag{20}$$

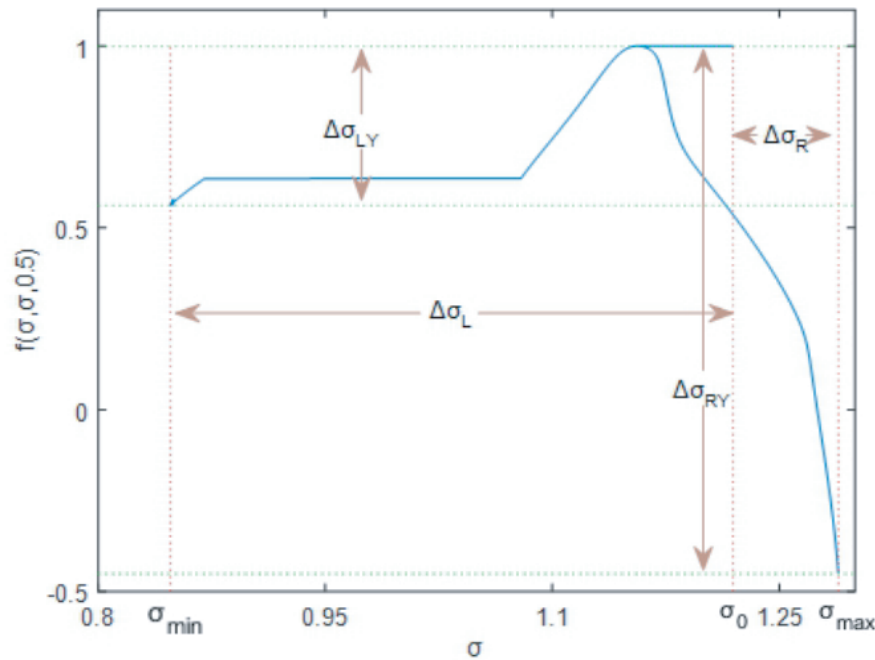
In the above formula,

$$\Delta\sigma_L = \sigma_0 - \sigma_{\min} \tag{21}$$

$$\Delta\sigma_R = \sigma_{\max} - \sigma_0 \tag{22}$$

wherein  $\sigma$  is the singularity index corresponding to the maximum value of the MFC spectrum.  $\sigma_{\min}$  is the minimum value of the singularity exponent.  $\sigma_{\max}$  is the maximum of the singularity exponent.

From the slice of the MFC spectrum on the plane, we can see the method to obtain the feature, as shown in Fig. 2.



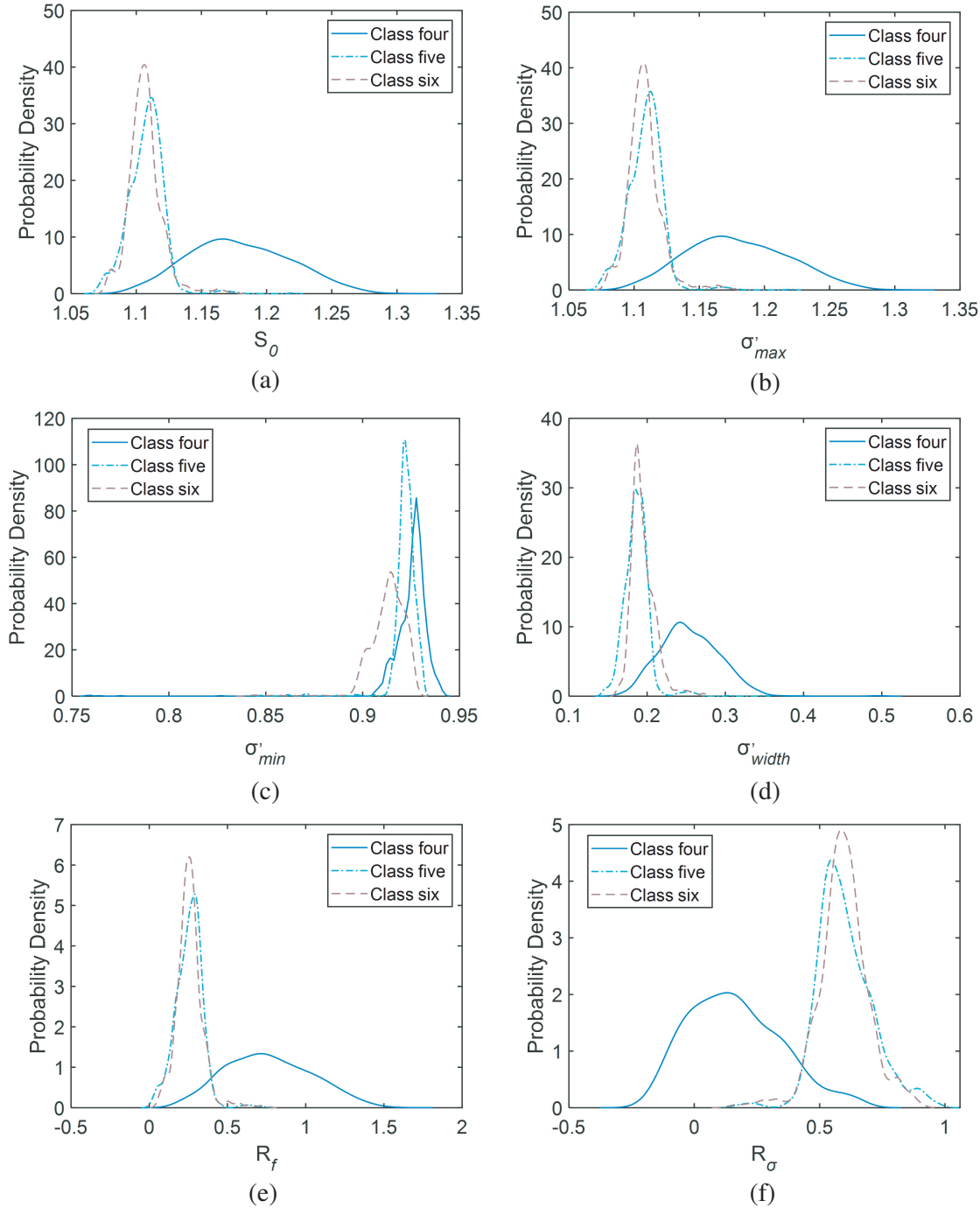
**Figure 2.** Slice of  $f(\sigma', \sigma'', w)$  in the  $\sigma' = \sigma''$  plane.

Figure 2 shows the slice of the MFC spectrum of a specific aircraft signal in the  $\sigma' = \sigma''$  plane. In the figure, we indicate the essential data needed to calculate the above six features, among which the critical data are  $(\sigma_{\min}, f(\sigma_{\min}, \sigma_{\min}, w))$ ,  $(\sigma_{\max}, f(\sigma_{\max}, \sigma_{\max}, w))$  and  $(\sigma_0, \max(f(\sigma', \sigma'', w)))$ . From the figure, we can see the characteristics of the signal from the distribution of  $\sigma$  and  $f(\sigma', \sigma'', w)$ .

### 3.4. Validity of Features

According to the six features defined above, we give the probability density distribution curve of echo MFC spectrum feature description parameters under the flight attitude of the back station.

As shown in Fig. 3, it is not easy to distinguish the three types of aircraft based on anyone feature. Figs. 3(a), (b), (d), (e), and (f) can easily distinguish the sixth type of aircraft targets. The figure most likely to distinguish between category four and category five is Fig. 3(c). Intuitively, although many MFC features overlap within a specific range, it is still possible to obtain better performance by comprehensively utilizing these features.



**Figure 3.** Probability density distribution curves of three MFC characteristic parameters. (a) Spectral barycenter. (b) The maximum singularity index. (c) The minimum singularity index. (d) Spectral correlation width. (e) Distribution width ratio. (f) Asymmetric index.

According to the purpose of classification, choosing the most stable characteristics of the classification object as the basis, and the basis of classification is the key to ensure the stability of the resulting classification results. It can be found that not all can effectively classify target characteristics. After a series of screening, we believe that using the maximum singularity index of MFC spectrum, the minimum singularity index of the MFC spectrum associated with MFC spectrum distribution width ratio can be obtained with the best effect. The following figures show the scatter distribution of three features at two angles.

Figure 4 shows the scatter distribution of these three MFC features. From perspective 1, it can be seen that the fifth and sixth classes are challenging to distinguish. However, from perspective 2, it can be found that there is still an obvious dividing line between the fifth class and sixth class. Therefore, aircraft targets can be classified effectively based on these three MFC features.

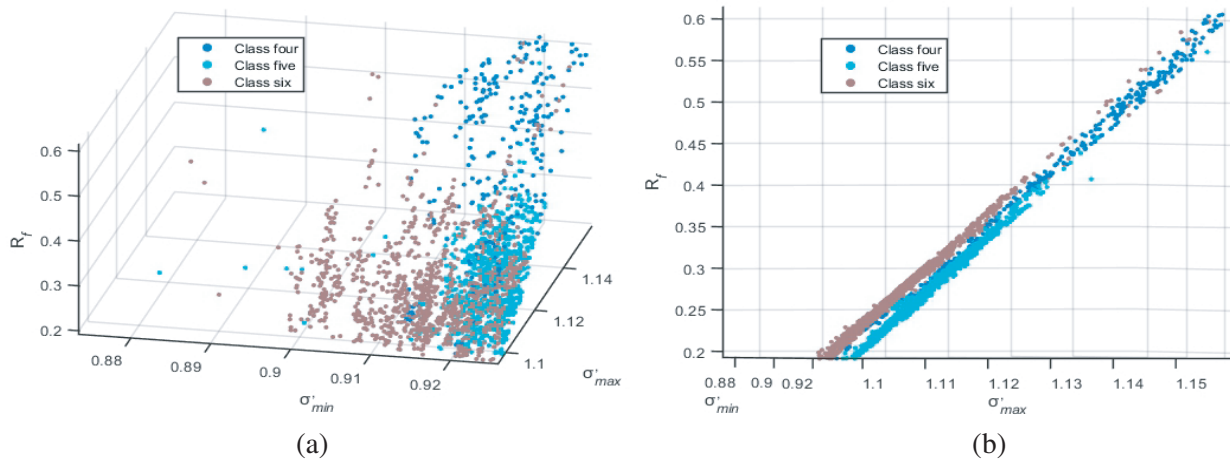


**Figure 4.** Scattering distribution of MFC spectrum characteristics under the flight attitude of the back station. (a) Perspective 1. (b) Perspective 2.

#### 4. EXPERIMENT AND ANALYSIS

##### 4.1. Experimental Data and Evaluation Indexes

The experimental data are the measured radar echo data of prominent civil aircraft, small civil aircraft and fighter aircraft. The first three types of data are aircraft flying towards the station, and the last three types of data are aircraft flying at the back station. The experimental data set consists of 7680 groups. Table 1 presents the statistical information of training and test samples, in which the order of training and test sets is randomly scrambled.

**Table 1.** Statistical information of training set and test set.

Experiments	Classes	Total sample	Training set	Test set
Towards the radar station	The first class	1280	1024	256
	The second class	1280	1024	256
	The third class	1280	1024	256
Off the radar station	The fourth class	1280	1024	256
	The fifth class	1280	1024	256
	The sixth class	1280	1024	256

There are four indicators in the classification task, namely: true positive (TP), false positive (FP), false negative (FN), and true negative (TN) [25].

(1) The probability that  $P$  (Precision) is a positive sample among all the predicted positive samples which is expressed as follows:

$$P = \frac{TP}{TP + FP} \quad (23)$$

(2) ACC (Accuracy) can measure the prediction accuracy of the classifier and is expressed in Eq. (24):

$$ACC = \frac{TP + TN}{TP + FP + FN + TN} \quad (24)$$

(3) ROC (receiver operating characteristic) curve can reflect the comprehensive index of sensitivity and specificity continuous variables [26]. Each point on the ROC curve reflects the sensitivity to the same signal stimulus. The horizontal and vertical coordinates of the ROC curve are FPR and TPR, respectively:

$$TPR = TP / (TP + FN) \quad (25)$$

$$FPR = FP / (FP + TN) \quad (26)$$

In addition, AUC (Area Under Curve) is defined as the area enclosed by the ROC Curve and the coordinate axis [27], which can be used to judge the ability of a classifier to identify samples at a certain threshold. The closer the AUC is to 1.0, the higher the authenticity of the detection method is.

## 4.2. Comparison Model

To evaluate the performance of the experimental method in this paper, tests will be conducted on the above data set and compared with the following methods:

(1) The classification method is based on multifractal (CMMF). From the perspective of MF, Liu and Zhang calculated the MF spectrum and realized the classification of rock mass quality [28].

(2) The classification method is based on EEMD and multifractal (CMEEMDMF). Hu et al. used EEMD to denoise radar echoes and then combined with MF to recognize civil aircraft and fighter aircraft [29].

(3) The classification method is based on multifractal correlation (CMMFC). Guan et al. introduced the MFC theory to analyze the characteristics of sea clutter time series and detect weak targets in the background of sea clutter [19].

(4) The classification method is based on fractional Fourier transform and multifractal correlation (CMFRFTMFC). Zhang and Li adjusted the signal-to-noise ratio of radar echo signals to the maximum by using fractional-order Fourier transform and classified aircraft echoes in this domain using the MFC theory [30].

## 4.3. Comparative Analysis of Experimental Results

Table 2 and Table 3 present the classification accuracy results based on ensemble empirical mode decomposition and multifractal correlation (CMEEMDMFC) and correlation comparison model on the unified data set. For the feature extraction process of various methods, the features in the original paper are preferred, and some features are modified according to the corresponding knowledge at the necessary time to optimize the practical effect. In the final classification, the support vector machine is used as the classification method. In Table 2 and Table 3, each row represents the prediction accuracy of each category under the corresponding model experiment conditions, and the item with the highest score in each row is marked in bold to indicate the best performance.

As shown in Table 1 and Table 2, for the first three types of aircraft, the accuracy and AUC of CMEEMDMFC are higher than or close to other algorithms, and it can obtain better classification performance. For the fourth class aircraft, the accuracy after CMEEMDMFC treatment is lower than that of CMEEMDMF, but the AUC is higher than or close to that of other algorithms. The accuracy and AUC of CMEEMDMFC are higher than or close to other algorithms for the fifth class aircraft. For the sixth class aircraft, the accuracy of CMEEMDMFC is slightly lower than that of CMMF and

**Table 2.** Classification accuracy of aircraft flying towards station attitude of each model.

	CMMF	CMEEMDMF	CMMFC	CMEEMDMFC	CMFRFTMFC
$P_{one}$	91.41%	<b>98.44%</b>	86.72%	<b>98.44%</b>	94.92%
$P_{two}$	96.48%	88.67%	91.80%	97.27%	<b>97.66%</b>
$P_{three}$	88.67%	90.63%	96.48%	<b>97.40%</b>	92.19%
ACC	92.18%	92.58%	91.67%	<b>96.88%</b>	94.92%
$AUC_{one}$	0.97	<b>1.00</b>	0.97	<b>1.00</b>	0.99
$AUC_{two}$	0.99	0.98	0.98	0.99	<b>1.00</b>
$AUC_{three}$	0.96	0.98	0.98	<b>1.00</b>	0.98

**Table 3.** Classification accuracy of aircraft flying off station attitude of each model.

	CMMF	CMEEMDMF	CMMFC	CMEEMDMFC	CMFRFTMFC
$P_{four}$	91.41%	<b>97.27%</b>	83.98%	94.14%	95.31%
$P_{five}$	82.03%	89.45%	95.31%	<b>99.22%</b>	91.02%
$P_{six}$	<b>99.22%</b>	87.50%	<b>99.22%</b>	97.66%	92.58%
ACC	90.89%	91.41%	89.32%	<b>97.01%</b>	92.97%
$AUC_{four}$	0.97	0.99	0.96	<b>0.99</b>	0.98
$AUC_{five}$	0.97	0.97	0.97	<b>1.00</b>	0.98
$AUC_{six}$	1.00	0.98	<b>1.00</b>	<b>1.00</b>	0.98

CMEEMDMF. The AUC of CMEEMDMFC is higher than or close to that of other algorithms. For CMEEMDMFC, ACC was around 97% for both attitude flight conditions. The ACC of other methods was around 92%. In general, the CMEEMDMFC model proposed in this paper is superior to the relevant models in the two groups of experiments. The results obtained in the two groups of experiments are close to the optimal model. The results show that the CMEEMDMFC model can effectively handle the aircraft classification task.

EEMD can decompose signals. In this paper, the waveform entropy is used to screen noise and improve the SNR of aircraft echo, which is helpful for aircraft classification. As can be seen from the first, third, fifth, and sixth classes, EEMD certainly works. Nevertheless for the second class and the sixth class EEMD is counterproductive. Therefore, this paper believes that there is a better screening method than waveform entropy, making all kinds of aircraft more easily identified. It is generally accepted that the results of MFC-based methods are better than MF-based methods. The MF spectrum is determined by statistical analysis of the singularity index on the support points of the fractal geometry observed. The MFC spectrum improves the single-point statistical feature of the MF spectrum into a two-point statistical feature. Therefore, it can better describe the physical structure difference of different types of aircraft targets. However, according to the experimental results, the accuracy of the first, second, fourth, and sixth classes, the MF is higher than or equal to MFC, possibly because noise has a more significant impact on the multi-fractal correlation characteristics.

Compared with CMEEMDMFC and CMFRFTMFC, both methods are experiments based on improving the SNR. However, CMEEMDMFC achieves its goal by removing the corresponding noise, while CMFRFTMFC achieves its goal by changing the performance of signals in different frequency domains. Whether from the experimental results or the theoretical perspective, it can be shown that the effect of CMEEMDMFC is better than or equal to CMFRFTMFC. However, when the model performance is judged in terms of time-consuming, the approach in this paper is not satisfactory. EEMD is a long process. MFC is also a time-consuming process. The experiment in this paper, takes about 3.6646 seconds to carry out EEMD for a set of data, about 6.5554 seconds to calculate MFC, and about 0.7230 seconds to search for the optimal phase fractional Fourier transform. The algorithm

in this paper is a model that takes the most time, which is also its shortcoming.

The confusion matrices obtained by the CMEEMDMFC experimental method are shown in Table 4 and Table 5.

**Table 4.** CMEEMDMFC confusion matrix for flying towards station attitude experiment.

	Class one	Class two	Class three
Class one	252	4	0
Class two	0	249	7
Class three	0	9	247

**Table 5.** CMEEMDMFC confusion matrix for flying off station attitude experiment.

	Class four	Class five	Class six
Class four	241	8	7
Class five	2	254	0
Class six	6	0	250

Finally, it must be mentioned that the EEMD parameter values used in this article are all suggested values given by the original author and are not necessarily suitable for this data set. If more appropriate parameters than the current experiment are selected, more accurate conclusions may be obtained. This paper also uses empirical values to screen the waveform entropy threshold. Better experimental results may be obtained if a more appropriate threshold is used. The features selected in this article are generally used and understood by the public. If the features are more profound than currently defined, the results may be better.

## 5. CONCLUSION

In this paper, an aircraft target classification and recognition model is proposed based on EEMD and MFC. By introducing EEMD and defining new features, this model can effectively improve the accuracy of aircraft target classification. The experimental results show that the classification algorithm can improve the SNR with the help of EEMD and help to highlight the characteristics of MFC; MFC characteristics can further emphasize that by selecting appropriate IMF recombination and waveform entropy threshold; the custom features can effectively express the characteristics of MFC, and then achieve feature extraction of aircraft targets. The experimental results show that the performance of the proposed model based on EEMDMFC on this data set is not entirely better than other current models, but the overall performance is better than the existing related work.

This article takes a long time to set thresholds and customize features. To reduce the consumption of time and improve the robustness of the model, in future work, we will focus on how depth research in the field of study can be incorporated into the current model. The features of fractal analysis are further extracted by deep learning to improve classification accuracy.

## ACKNOWLEDGMENT

The authors would like to thank the National Natural Science Foundation of China (Grant: 61561004) for supporting this research work and also wish to thank the anonymous reviewers for their help in improving this paper.

## REFERENCES

1. Long, T., Z. Liang, and Q. Liu, "Advanced technology of high-resolution radar: Target detection, tracking, imaging, and recognition," *Science China Information Sciences*, Vol. 62, No. 04, 2019.
2. Yang, X., "Building detection from high-resolution polarimetric SAR images," University of Electronic Science and Technology of China, 2017.
3. Zhang, G., R. Li, and D. Wang, "A review of low-resolution radar target classification methods," *Digital Communication World*, Vol. 05, 280, 2018.
4. Ding, J. and X. Zhang, "Jet engine modulation signatures of propeller aircraft in air-defense radar signals," *Journal of Tsinghua University (Science and Technology)*, Vol. 03, 418–421, 2003.
5. Wang, B., "Study on classification of airplane targets based on micro-Doppler effect," Xidian University, 2015.
6. Yang, W., et al., "Automatic feature extraction from insufficient JEM signals based on compressed sensing method," *2015 Asia-Pacific Microwave Conference*, Vol. 02, 1–3, 2016.
7. Ebrahimi, S., et al., "Iris recognition system based on fractal dimensions using improved box counting," *Journal of Information Science and Engineering*, Vol. 35, No. 02, 275–290, 2018.
8. Silva, P. M. and J. B. Florindo, "Fractal measures of image local features: An application to texture recognition," *Multimedia Tools and Applications*, Vol. 80, 14213–14229, 2021.
9. Ni, J., et al., "Target classification of low-resolution radar based on fractional brown feature," *Modern Radar*, Vol. 33, No. 06, 46–48, 2011.
10. Li, Q. and W. Xie, "Target classification with low-resolution surveillance radars based on multifractal features," *Progress In Electromagnetics Research B*, Vol. 45, 291–308, 2012.
11. Li, Q. and W. Xie, "Research on analysis of multifractal correlation characteristics of aircraft echoes and classification of targets in surveillance radars," *Progress In Electromagnetics Research B*, Vol. 54, 27–44, 2013.
12. Zhang, H., Q. Li, C. Rong, and X. Yuan, "Target classification with low-resolution radars based on multifractal features in fractional Fourier domain," *Progress In Electromagnetics Research M*, Vol. 79, 51–60, 2019.
13. Qu, Z., X. Mao, and C. Hou, "Radar signal recognition based on singular value entropy and fractal dimension," *Systems Engineering and Electronics*, Vol. 40, No. 02, 303–307, 2018.
14. Chen, C., et al., "A new method for sorting unknown radar emitter signal," *Chinese Journal of Electronics*, Vol. 23, No. 03, 499–502, 2014.
15. Huo, Y., Y. Fang, and X. Long, "Lightning electric field signals recognition based on EMD and fractal theory," *Journal of Northwest Normal University (Natural Science)*, Vol. 55, No. 05, 33–38+50, 2019.
16. Wang, R., M. Xiang, and C. Li, "Denoising FMCW radar signals via EEMD with singular spectrum constraint," *IEEE Geoscience and Remote Sensing Letters*, 1–5, 2019.
17. Li, C., et al., "Fault diagnosis of rolling element bearing of correlation coefficient and arrangement entropy based on EEMD," *Modular Machine Tool & Automatic Manufacturing Technique*, Vol. 08, 1–4, 2020.
18. He, J. and J. Xu, "The multifractal spectrum of a sea clutter using a random walk model," *Acta Oceanologica Sinica*, Vol. 36, No. 09, 23–26, 2017.
19. Guan, J., et al., "Multifractal correlation characteristic of real sea clutter and low-observable targets detection," *Journal of Electronics & Information Technology*, Vol. 32, No. 01, 54–61, 2010.
20. Wu, Z. and N. E. Huang, "Ensemble empirical mode decomposition: A noise-assisted data analysis method," *Advances in Adaptive Data Analysis*, Vol. 01, No. 01, 1–41, 2009.
21. Zhang, Z., Y. Du, and W. Hu, "Waveform entropy-based target detection in HRRPs," *Aeronautical Computing Technique*, Vol. 06, 51–54, 2007.
22. Li, Q., H. Zhang, Q. Lu, and L. Wei, "Research on analysis of aircraft echo characteristics and classification of targets in low-resolution radars based on EEMD," *Progress In Electromagnetics Research M*, Vol. 68, 61–68, 2018.

23. Yang, H., Y. Cheng, and G. Li, "A denoising method for ship radiated noise based on Spearman variational mode decomposition, spatial-dependence recurrence sample entropy, improved wavelet threshold denoising, and Savitzky-Golay filter," *Alexandria Engineering Journal*, Vol. 60, No. 03, 3379–3400, 2021.
24. Zhang, H. and Q. Li, "Target classification based on multifractal features in fractional Fourier transform domain," *Radar Science and Technology*, Vol. 17, No. 06, 647–654, 2019.
25. Gerdan, D., A. Beyaz, and M. Vatandas, "Classification of apple varieties: Comparison of ensemble learning and naive bayes algorithms in H<sub>2</sub>O framework," *Journal of Agricultural Faculty of Gaziosmanpasa University*, Vol. 37, No. 01, 9–16, 2020.
26. Rao, B., et al., "ACPred-Fuse: Fusing multi-view information improves the prediction of anticancer peptides," *Briefings Bioinformatics*, Vol. 21, No. 05, 1846–1855, 2020.
27. Lobo, J. M., A. Jiménez-Valverde, and R. Real, "AUC: A misleading measure of the performance of predictive distribution models," *Global Ecology and Biogeography*, Vol. 17, No. 02, 145–151, 2008.
28. Liu, S. and F. Zhang, "Multifractal evaluation and classification of 3-D jointed rock mass quality," *Rock and Soil Mechanics*, Vol. 07, 1116–1121, 2004.
29. Hu, J., Q. Li, Q. Zhang, and Y. Zhong, "Aircraft target classification method based on EEMD and multifractal," *Progress In Electromagnetics Research M*, Vol. 99, 223–231, 2021.
30. Zhang, H. and Q. Li, "Target classification with low-resolution radars based on multifractal correlation characteristics in fractional Fourier domain," *Progress In Electromagnetics Research C*, Vol. 94, 161–176, 2019.